Military Technical College
Kobry El-Kobbah,
Cairo, Egypt.

13th International Conference
on Applied Mechanics and
Mechanical Engineering.

AIR FLOW PATTERNS IN AN AIR CONDITIONED MEASURING EQUIPMENT LABORATORY

FARAG* A.M., KHALIL** E.E. and MORKOS** S. M.

ABSTRACT

Calibration for the measuring instruments in the Air Force Measuring Equipment Laboratories, are considered to be one of the reasons for flight success in Egyptian Air Force. Hence, they should be preserved from the different factors that might cause harm or decrease the accuracy in calibration for the measuring instruments. One of these factors is the excessive relative humidity as it affects the mechanical and physical properties of the standard instruments that are considered the reference. Measuring instruments need to be calibrated from time to time to provide high accuracy in use that occurs by comparing a measuring device (uncalibrated) against an equal or better standard.

The present paper focuses on the heat transfer interactions on the air flow in Precision Measuring Equipment Laboratories (PMEL). Many PMELs built or renovated in recent years have not met minimum operating environment standards. The impact of flow parameters on the air flow pattern were investigated. This offers the designer a better view of design limits to enable him to adequately select the optimum design from a wide number of alternative options and to use them in forecasting and even monitoring. Air movement inside enclosures prediction via CFD is a strong tool for reaching better designs for inlets and outlets positions in ventilated spaces. Fluent Computational Software [1] was used to predict the parameters affecting the air distribution inside air-conditioned spaces. Continuity, momentum, energy, and species transport equations in addition to k-epsilon model equations for turbulence closure were solved using finite volume method. Furthermore the paper includes full-scale actual existing space experiments, to obtain good documented full-scale measurements in actual ventilated laboratory room that can be used for comparison with CFD-simulations.

Many of the reported comparisons were found in good agreement with experiments and aided the assessment of the numerical procedure application to air-conditioned spaces. Finally, it was found that the optimum airside system design should allow the air to pass all the enclosure areas before being extracted. Temperature and humidity control are crucial elements of laboratory design. Since temperature fluctuations also affect humidity, its control is especially important. Also a restriction should be made for the mechanical and optical disciplines, the internationally accepted temperature is not exceed 20°C.

KEY WORDS: Air-conditioned, Calibration, Measuring, Equipment, CFD.

----

*   Egyptian Air Force.
**   Mechanical Power Engineering Department , Faculty of Engineering, Cairo University, Cairo, Egypt.

NOMENCLATURE

Symbol	Quantity
ρ	Density, kg/m^3
C	Constant
V	Computational cell Volume, m^3
d	Distance, m
RH	Relative humidity, %
T	Temperature, K
E	Total energy of a fluid particle, J Dimensionless term describing the turbulent dissipation rate, ε
u	Instantaneous velocity component in x direction, m/s
U	Axial velocity, m/s
t	Time, s
G_b	Generation of turbulent kinetic energy, k, due to boyancy
G_k	Turbulence kinetic energy production
Gr	Grashohf number, $Gr_L = \dfrac{g\beta(T_s - T_\infty)L^3}{v^2}$
h	Enthalpy, kJ/kg
μ	Molecular viscosity, kg.m/s
H	Height, m
Br	Brinkman number, $\mathrm{Br} = \dfrac{\mu U_e^2}{k\Delta T}$
S	Source term modulus of the mean rate-of-strain tensor
k	Turbulent Kinetic energy, m^2/s^2 Thermal conductivity, W/m^{o}c
$\vec{v}$	Velocity vector, m/s
v	Velocity magnitude, m/s Instantaneous velocity component in y direction, m/s
w	Instantaneous velocity component in z direction, m/s
S	Source term modulus of the mean rate-of-strain tensor
Nu	Nusselt number, $Nu_L = \dfrac{hL}{k_f}$
p	Pressure, Pa
Pr	Prandtl Number, $Pr = C_p \mu / k$
Ra	Rayleigh number, Ra = Gr × Pr
Re	Reynolds Number, Re = ρ U l / μ
x, y, z	Cartesian coordinate components
eff	Effective property
ε	Turbulence dissipation rate m^2/s^3
Γ	Diffusivity
ϕ	Donates Scalar property (i.e. density, energy, ..etc.)

INTRODUCTION

The introduction of a proper ventilation system was suggested in order to control the indoor air climate conditions. Proper ventilation system is very necessary to satisfy the precision in calibration for the Measuring Equipment Laboratory. Ventilation in this kind of critical applications has not been investigated before. That is why this research aims to find the optimum airside system design through CFD simulation as well as to develop adequate understanding of the problem. Air movement inside enclosures prediction via CFD is a strong tool for reaching better designs for inlets and outlets positions in ventilated spaces.

The objectives of this paper are studying and understanding the nature of the give air flow problem:
- To explore the options for measurement of indoor air flow patterns, with respect to accuracy, sensitivity, applicability and availability,
- To obtain good documented full-scale measurements in actual ventilated laboratory room that can be used for comparison with CFD-simulations.
- To investigate a type of flow problem that subscribes to the current view in ventilation.

The previous experimental and numerical investigations of airflow characteristics in the enclosed spaces have been reviewed to provide an overall view of the research status at the start of the present work , Such as Yamazaki, et al. [2], covered the physical modelling using a full-scale model and also the mathematical modelling. They constructed a system of air distribution in an air-conditioned space, then by using the algorithm of Launder and Spalding [3] , and that modified by Spalding and Patankar [4], they solved the three dimensional distribution of flow and temperature in the desired space. They also compared the computed results with the experimental data; and reported some of differences between the computed and the experimental results.

Medhat [5] performed a comprehensive set of flow and heat transfer measurements on the reduced-scale model of a conference room. He found that reduced-scale model can yield representative indications only in simple configurations. Hosni et al [6] performed an experimental investigation to measure flow characteristics in a conference room and reported also the corresponding numerical investigation. Medhat [7] performed flow and heat transfer experiments on the full-scale model of a conference room. He found that the turbulence nature of the flow is normally non-isotropic in all cases of experimental tests. The buoyant forces with non-isothermal jet cause the throw to be shorter than that in the isothermal jet for velocities less than 0.762 m/s. Nielsen [8] studied the fluid flow characteristics in the air-conditioned room configuration of Blum [9]. (H denotes the room height; room length is 3H, room width is 2H. The inlet (supply) /wall area ratio is 0.00126; thus yields inlet Reynolds number of 93000).

Kameel and Khalil [10] studied the velocities, turbulence distributions and heat transfer interactions inside a conference room. They studied the effects of supply flow rate, discharge velocity, supply area, and discharge angel on the airflow and temperature distribution inside the conference room. They concluded that airflow patterns in rooms are more quite using longer supply grilles and both micro and macro mixing levels are influential. More maximum absolute velocities and higher turbulent characteristics are demonstrated in situations with smaller supply jets where cold jet penetrates more.

Gaspar et al. [11] evaluated the performance of different CFD codes in building and environmental analysis. The advantages and the performance of (two) commercial CFD codes and an academic CFD code developed for this purpose are evaluated. The codes were applied to predict typical situations of the airflow in buildings and the predictions were compared with experimental results. A reduced scale model was used for experimental investigations. The comparison between numerical and experimental results showed much more agreement for the velocities than for the temperatures. Schälin and Nielsen [12] studied the validity of turbulence models for the computational fluid dynamics simulation for airflow inside enclosures. They have concluded that the well-established k-ε model shows large deviations in the occupied zone. And hence this turbulence model needs further improvements. They have found also that the wall jet behaviour can be conveniently modelled using a suited wall reflection terms in the Reynolds-averaged Navier-Stokes (RANS) models, these can be included in the RSM, and the algebraic stress models (ASM). Finlayson et al. [13], used computational fluid dynamics commercial package in order to predict the pollutant dispersion in a large indoor space . Comparison with a scale model experiment for isothermal flow of a previous work by Thatcher et al. was also investigated and analyzed. The results suggest that computational fluid dynamics modelling approach is adequate for predicting isothermal pollutant transport in a large room with simple geometry. Their work assumed that "agreement between CFD predictions and ensemble averaged experimental measurements is quantified using the ratios of CFD-predicted and experimentally measured dye concentration at a large number of points in the measurement plane". The results of the investigations were considered good as these ratios fall between 0.5 and 2.0 at all points in the plane. The standard k-epsilon two-equation turbulence model obtains this level of agreement and predicts pollutant arrival time to the measurement plane within a few seconds.

This paper consists of both experimental and numerical approaches to predict the flow pattern in the vicinity of supply diffusers and in the vicinity of the level of standard devices (level of operator) for measuring the instruments, and the comparison between them. An experimental traversing mechanism and experimental robust measuring probes were utilized to measure and map the velocity, temperature and relative humidity contours.

COMPUTATIONAL WORK

For this paper, CFD simulation for airflow inside a laboratory room, numerical techniques were used to model the airflow characteristics. This refers to the mathematical modeling and analysis of the movements of fluids (liquids or gases) under specified conditions to predict behavior. Because the calculations are so extensive and repetitive, CFD analysis requires the use of a powerful computer. Graphical output shows the results of the analysis.

Governing Equations

The program solves the differential equations governing the transport of mass, three momentum components, and energy in 3D configurations under steady conditions [14-19].

The different governing partial differential equations are typically expressed in a general form as:

$$\frac{\partial}{\partial x}\rho U\Phi + \frac{\partial}{\partial y}V\Phi + \frac{\partial}{\partial z}W\Phi = \frac{\partial}{\partial x}\left(\Gamma\Phi,\text{eff}\ \frac{\partial\Phi}{\partial x}\right) + \frac{\partial}{\partial y}\left(\Gamma\Phi,\text{eff}\ \frac{\partial\Phi}{\partial y}\right) + \frac{\partial}{\partial z}\left(\Gamma\Phi,\text{eff}\ \frac{\partial\Phi}{\partial z}\right) + S_\Phi \dots (1)$$

Where: ρ = Air density, kg/m3
Φ = Dependent variable.
S_Φ = Source term of Φ.
U, V, W = Velocity vectors.
$\Gamma_{\Phi,\ \text{eff}}$ = Effective diffusion coefficient.

The effective diffusion coefficients and source terms for the various differential equations are listed in Table1. Turbulence model of Launder et al [3] was incorporated in this paper. Details of the modeling technique and assumptions can be found in references [3], [8], [10], [20], and [21].

Computational Domain

The results of the numerical prediction and the corresponding analysis are presented in this paper, including the influence of supply air temperature, supply air velocity, outlet shape on the main air parameters, such as air throw, airdrop, room air velocity, temperature distribution, and influence of return air. The room height (H) is 3.0 m, the room width (W) is 8.0 m, and the room length (L) is 13.0 m. The supplied airflow to the laboratory was deviced through three square ceiling perforated diffusers each 0.6 x 0.6 m. The air extract system in the laboratory is based on the extract of the flow from two square ceiling extract grills (Return Openings),(R1,R2), each 0.6 * 0.6 m, The two extract grills centers are located at X, Y equal to (2.4,10.7)m, and R2 is located at (6.6,7.7)m. The three supply diffuser centers are located at X, Y equal to (1.4, 7.7), (2.4, 6.5), (6, 6.5), dimension in meters. Such design was developed to isolate the region of operation from the all environment in the laboratory. The present experiments were performed with the presence of two standard devices (D1 , D2) used for calibrating the instruments, whose dimensions are (0.7*0.6*0.15 m), each of them has heat flux =1kW/m2 , D1 is located at X, Y, Z equal to (1.5,3,1)m, and D2 is located at X, Y, Z equal to (5.9,10,1)m, as shown in Fig.1.

Numerical Solution Techniques

Mesh sizes used in this paper exceeded 200,000 mesh volumes in one case, and all mesh sizes were above 600,000 mesh volumes which allowed better and meaningful predictions of the flow regimes. The SIMPLE algorithm is used for the pressure-velocity coupling and a second order upwind scheme was use for discretization of the governing equations.

The governing equations are solved simultaneously with thermal boundary conditions, hydrodynamics, and turbulence model enable to predict the air flow characteristics quantitatively.

Table 1. Terms of Partial Differential Equations (PDE).

	Φ	$\Gamma_{\Phi,eff}$	S_Φ
Continuity	1	0	0
X-momentum	U	μ_{eff}	$-\partial P/\partial x + \rho g_x$
Y-momentum	V	μ_{eff}	$-\partial P/\partial y + \rho g_y(1+\beta\Delta t)$
Z-momentum	W	μ_{eff}	$-\partial P/\partial z + \rho g_z$
H-equation	H	μ_{eff}/σ_H	.... S_H
k-equation	k	μ_{eff}/σ_k	$G - \rho\varepsilon$
ε-equation	ε	$\mu_{eff}/\sigma_\varepsilon$	$C_1\varepsilon G/k - C_2\rho\varepsilon_2/k$

$\mu_{eff} = \mu_{lam} + \mu_t$ $\qquad\qquad$ $\mu_t = \rho C_\mu k_2/\varepsilon$

$G = \mu_t[2\{(\partial U/\partial x)^2 + (\partial V/\partial y)^2 + (\partial W/\partial z)^2\} + (\partial U/\partial y + \partial V/\partial x)^2 + (\partial V/\partial z + \partial W/\partial y)^2 + (\partial U/\partial z + \partial W/\partial x)^2]$

$C_1 = 1.44$, $C_2 = 1.92$, $C_\mu = 0.09$
$\sigma_H = 0.9$, $\sigma_{RH} = 0.9$, $\sigma_\tau = 0.9$, $\sigma_k = 0.9$, $\sigma_\varepsilon = 1.225$

Boundary Conditions

The flow field is taken as a stagnant field initially which led to make the initial values of U, V and W equals to zero. Fluctuations in the velocities with intensity equal to 1 % of the inlet velocity of air are assumed. This leads to calculate the initial kinetic energy k and the initial dissipation rate ε, that lead us to specify the k=0.0002 for normal velocities. The inlet velocity profiles are taken to have a uniform distribution. The inlet fluctuations in the inlet velocity are taken with intensity equal to 0.2 of the inlet velocity, and to be uniform in form. The corresponding exit flow conditions are similar in the form to the inlet conditions.

The temperature conditions , which have a value in present cases. In cooling conditions the supply temperature will remain at constant value, and the room temperature will remain at constant temperature, which it is the initial condition. At the outlet opening, the condition will be taken as ($\partial t/\partial x$=0). A staggered grid system is employed for the velocities in the Z direction to avoid the decoupling effects between the velocity and the pressure that are frequently observed with the non staggered grid. The using of the staggered grid reduces the error in the calculation that being due to the closing of the air opening to the ceiling or the floor.

In the regions near a wall, the velocities tend to zero and hence the local Re is small, and if the exact momentum equations are to be solved in this region, then a large number of grid nodes is needed. One can resort to the alternative solution of "laminarizing" the model in these regions, as in Khalil 1978. The flow in the region near the wall is presented by the approximated Couettee flow based on the logarithmic law of the wall.

EXPERIMENTAL WORK

Measurements of the velocity, air temperature, and relative humidity were obtained in the present flow configuration with the aid of a (Hot-Wire Thermo-Anemometer).The present measuring setup comprises a three dimensional traverse mechanism was utilized to hold the measuring instrument at various locations in the room as shown in the schematic sketch in Fig.2.That traverse mechanism was designed and constructed from a connection of two sliding rods relative to each other. The lower rod is hollow and was supported over a rolling base , and The upper rod was designed to slide inside the lower rod. The height of the lower rod is 1.25 m from the floor and the height of the upper one is 1.85 m, and 1.75 m from the lower end of the lower rod; thus finally enabling a final possible height equals to 3.0 m from the floor.

The present measurements were performed in vicinity of supply diffusers, to obtain the complete data of inlet boundary conditions, also in the vicinity of the level of standard devices for measuring the instruments, to obtain the complete data about the conditions in the operating area. On the other hand, the same data will be used to verify the numerical procedure that will be produced to obtain more parametric simulations that assist to enhance our knowledge of the air environment inside the laboratory room.

Measurements were obtained in the vicinity of the supply grilles by dividing the measuring locations to 8 x 8 points at Z equal to 2.95 m, 2.9 m, 2.8 m, and 2.7 m, as shown in Fig.3. The measuring locations were distributed in Figure 3.4 such as to get optimum measuring results, and to minimize the experimental errors due to the position deviation uncertainty.

Measurements were obtained in the vicinity of the level of standard devices for measuring the instruments between 1.0 m height and 2.0 m height from the floor. Fig.4 shows the measuring locations in both horizontal and vertical sections.

RESULTS AND DISCUSSIONS

Table 2 illustrates the condition of non-isothermal cases (cooling processes) that achieved by using the present models and illustrate the output results that represented from it. Temperature difference Δt = -10°C, the inlet temperature t_0 = 15°C, and the outlet temperature (or Room temperature) t_r = 25°C. The dimension was tacked as (L,W, H equals 13.0,8.0,3.0 m), and the dimensions of the return openings (R1,R2) were tacked as (0.6 * 0.6m), and the angle of inlet air (Air Supply Outlet) was tacked as 30 angle downward to the horizontal (+ ve X direction). The supply air was introduced with a velocity equal to 0.9 m/s. The discharge angle equal to zero.

Table 2. Case Study.

	Case 1-NI
Supply Open (S1) m*m	0.6*0.6
Supply Open (S2) m*m	0.6*0.6
Supply Open (S3) m*m	0.6*0.6
Room Lengh (L) m	13
Mesh Size	600,000
Velocity Vector in vertical plan	Yes
Velocity Vector in horizontal plan	Yes
Velocity Contour in vertical plan	Yes
Velocity Contour in horizontal plan	Yes
Kinetic Energy Contour in horizontal plan	Yes
Relative Humidity Contour in horizontal plan	Yes
Isothermal Contour in horizontal plan	Yes

Figure 5 shows the predicted fluid flow vectors (in the horizontal plan). It can be seen that the small penetration of the inlet air, and the recirculation zone that created in the sides of the jet flow. The values of the reverse flow are relatively small to the main flow. The air penetration in this case was decreased strongly relatively to the isothermal cases, due to the presence of the buoyancy effect. In this case, the decreasing of inlet velocity, with comparing to the isothermal cases, has much effect on the air throw due to the combination of it with the presence of the temperature difference.

Figure 6 shows the predicted U velocity contour (constant velocity lines In the horizontal plan). The spread became small due to the high drop that caused due to the buoyancy effect. The jet recirculation zones were disappeared partially due to the high drop with the comparing to the isothermal cases.

Figure 7 shows the predicted isothermal contour (constant temperature lines in the horizontal plan). It can be seen the distribution of temperature in the room ,the temperature still constant and equal to the room temperature.

Figure 8 shows the predicted isothermal contour (constant temperature lines in the horizontal plan). It can be seen the distribution of temperature in the room ,the temperature still constant and equal to the room temperature, and the temperature near the devices is high due to the heat generation from them.

Figure 9 shows the predicted relative humidity (R.H.%) contour (constant relative humidity lines in the horizontal plan). It can be seen the higher humidity level appears in the ceiling below the supply openings that in the same region of the high velocity flow or by another words in the domain of the jet downstream, Hosni et al 1996.

Figure 11 shows the predicted relative humidity (R.H.%) contour (constant relative humidity lines in the horizontal plan). It can be seen the lower humidity level appears in the area around the devices that in the same region of the low velocity flow .

CONCLUSIONS

The following are the more important findings in this paper :
- Fluent is able to predict there are good agreement between numerical and experimental results.
- Small variation occurred in temperature and relative humidity in the laboratory room, which is required to satisfy the optimum conditions for calibration process.
- Fluid flow computations utilizing k - ε turbulence model are very sensitive to the inlet conditions assumptions, especially the kinetic energy (k) profile.

REFERENCES

[1]   FLUENT 2005, CFD CODE Manual, (2005).

[2]   Yamazaki, K., Komatsu, M., and Otsubo, M. "Applications of Numerical Simulation for Residential Room Air Conditioning" ASHRAE Trans. v. 93, (1990).

[3]   Launder, B.E., and Spalding, D.B., The numerical computation of turbulent flows, Computer Methods App. Mech., pp. 269-275,(1974).

[4]   Spalding, D. B., and Patankar, S. V., "A Calculation Procedure For Heat, Mass and Momentum Transfer in Three-Dimensional Parabolic Flows." Int. J. Heat & Mass Transfer, Vol. 15, pp. 1787, (1974).

[5]   Medhat, A.M. "Air Conditioning Flow Patterns in Enclosures", M.Sc. Thesis, Cairo University, (1993).

[6]   Hosni, M. H., Tsai, K., and Hawkins, A. N., "Numerical Prediction of Room Air Motion" Fluids Engineering Division Conference. V 01. ASME, pp. 745 -751, (1996).

[7]   Medhat, A. A., Optimizing room comfort using experimental and numerical modeling, Ph.D. Thesis, Cairo University, (1999).

[8]   Nielsen, P.V. , Numerical prediction of air distribution in rooms, ASHRAE, Building systems: room air and air contaminant distribution, (1989).

[9]   Blum, H. M., "Experimental Verification of Turbulence Models" ASHRAE Fundamentals vol. 1 pt. 30 published by ASHRAE, Atlanta, USA, (1956).

[10]   Kameel, R., and Khalil, E.E., Generation of the grid node distribution using modified hyperbolic equations, 40th Aerospace Sciences Meeting & Exhibit, Reno, Nevada, AIAA-2002 -656, (2002).

[11]   Pedro Dinis Gaspa, Rui F. Barroc and Pitamara R.A., "Performance Evaluation of CFD Codes in Building Energy and Environmental Analysis", Eighth International IBPSA, Conference ELindhoven, Netherlands August 11-14, (2003).

[12]   Schalin A. and Nielsen. P. V., "Impact of Turbulence Anisotropy Near Walls in Room Airflow". INDOOR AIR, Volume 14, (2004).

[13]   F'inlayson E. D., Gadgil A. J., Thatcher T. L., and Sextro R. G., "Pollutant Dispersion in a Large Indoor Space. Part 2: Computational Fluid Dynamics Predictions and Comparison with a Scale Model Experiment for Isothermal Flow". INDOOR AIR, Volume 14, (2004).

[14]   Olesen, B. W., Guidelines for comfort, ASHRAE Journal, pp. 41 - 46, (2000).

[15]   ISO EN 7730, Moderate thermal environments – Determination of the PMV and PPD indices and specification of the conditions for thermal comfort, International Standards Organization, Geneva, (1994).

[16]   Berglund, L. G., Comfort and humidity, ASHRAE Journal, pp.35 - 40, (1998).

[17]   Fang, L., Clausen, G., and Fanger, P. O., The impact of temperature and humidity on perception and emission of indoor air pollutants, Indoor Air' 96, Tokyo, Institute of Public health, (1996).

[18]   Tanabe, S., Kimura, K., and Hara, T., Thermal comfort requirement during the summer season in Japan, ASHRAE Transactions, 93(1): pp.564-577, (1987).

[19]   Kameel, R.,Computer aided design of flow regimes in air-conditioned operating theatres, Ph.D. Thesis work, Cairo University, (2002).

[20]   Khalil, E. E., Numerical Procedures as a tool to Engineering Design, Proc. Informatica 78, Yugoslavia , (1978).

[21]   Khalil, E. E., Fluid Flow Regimes Interactions in Air Conditioned Spaces, Proc. 3 rd Jordanian Mech. Engineering Conference, pp. 79, Amman, (1999).

S1........Supply Opening 1
S2........Supply Opening 2
S3........Supply Opening 3
R1........Return Opening 1
R2........Return Opening 2
D1........Standard Device 1
D2........Standard Device 2
L1.........Florocent Lamps 1
L2.........Florocent Lamps 2
L3.........Florocent Lamps 3
W1.......Glass Window 1
W2.......Glass Window 2
W3.......Glass Window 3
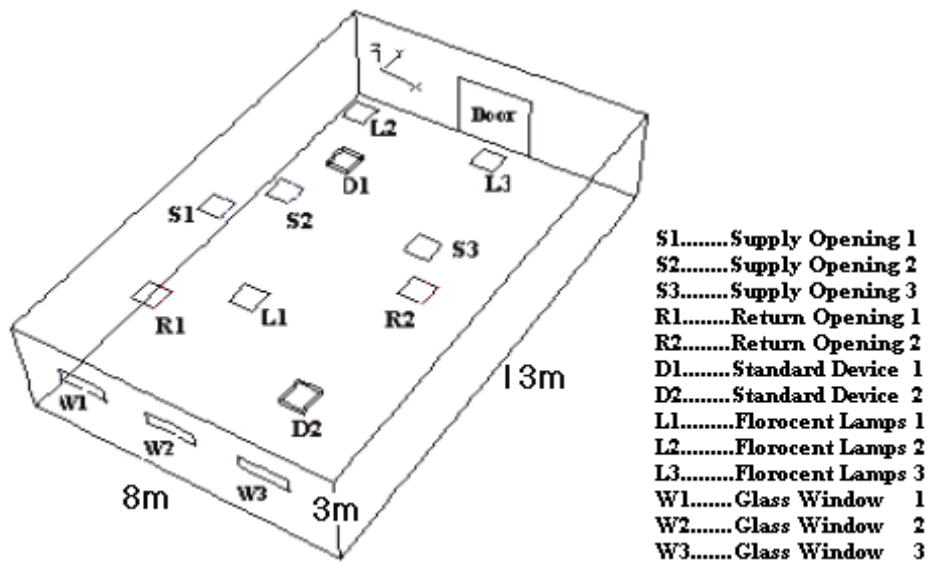
Fig.1. Laboratory Room Description
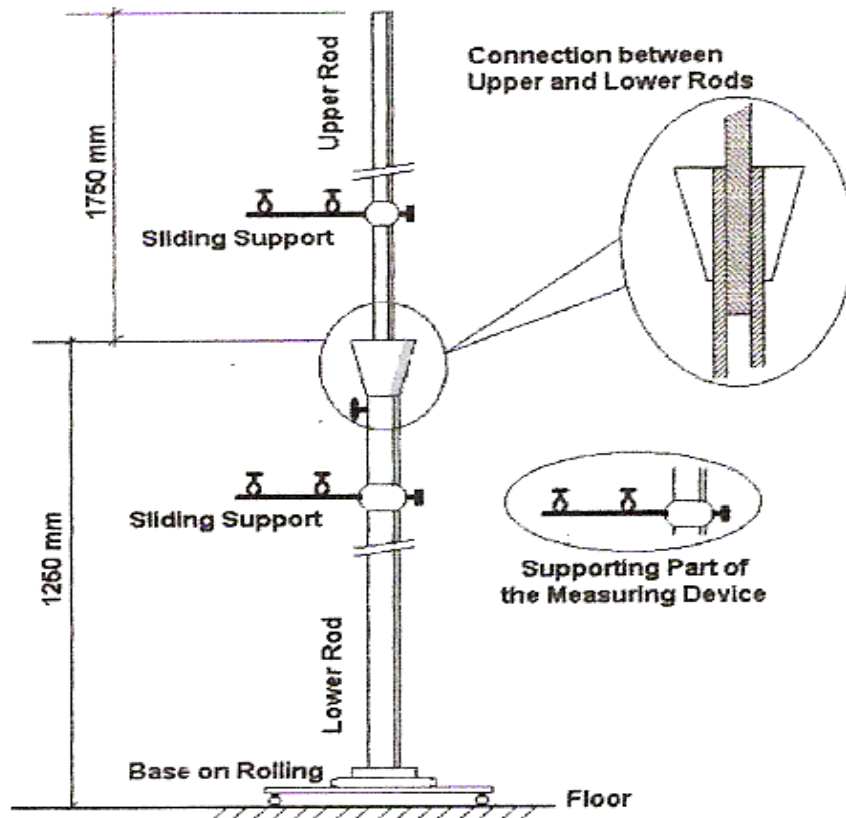
Fig .2. Schematic Sketch of the Traverse Mechanism to Hold the Measuring Instruments.
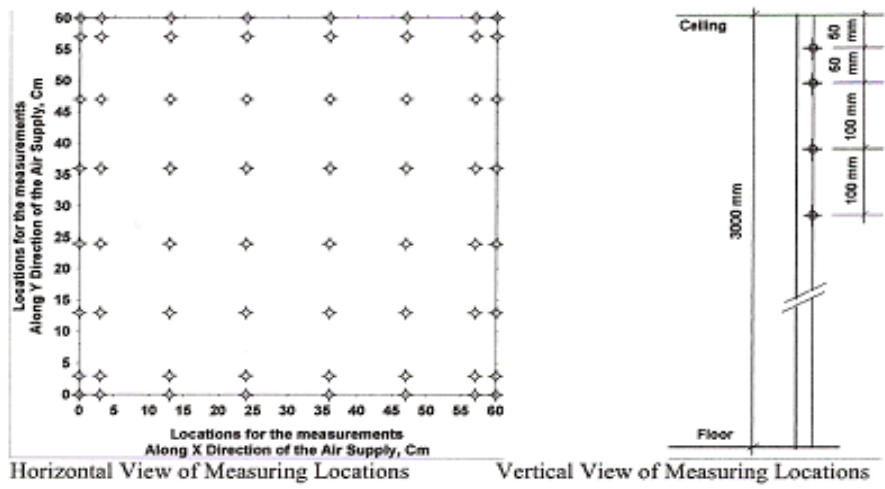
Fig.3. Measuring Locations.

Fig.4. Measuring Locations**.**

Velocity Vectors Colored By Velocity Magnitude (m/s)

Jan 19, 2007
FLUENT 6.2 (3d, segregated, spe, ske)
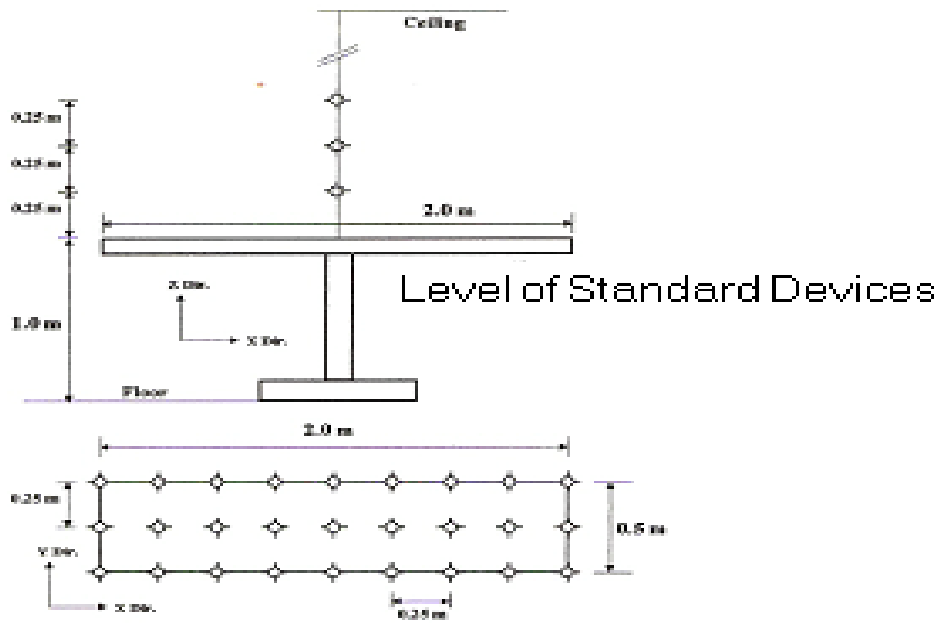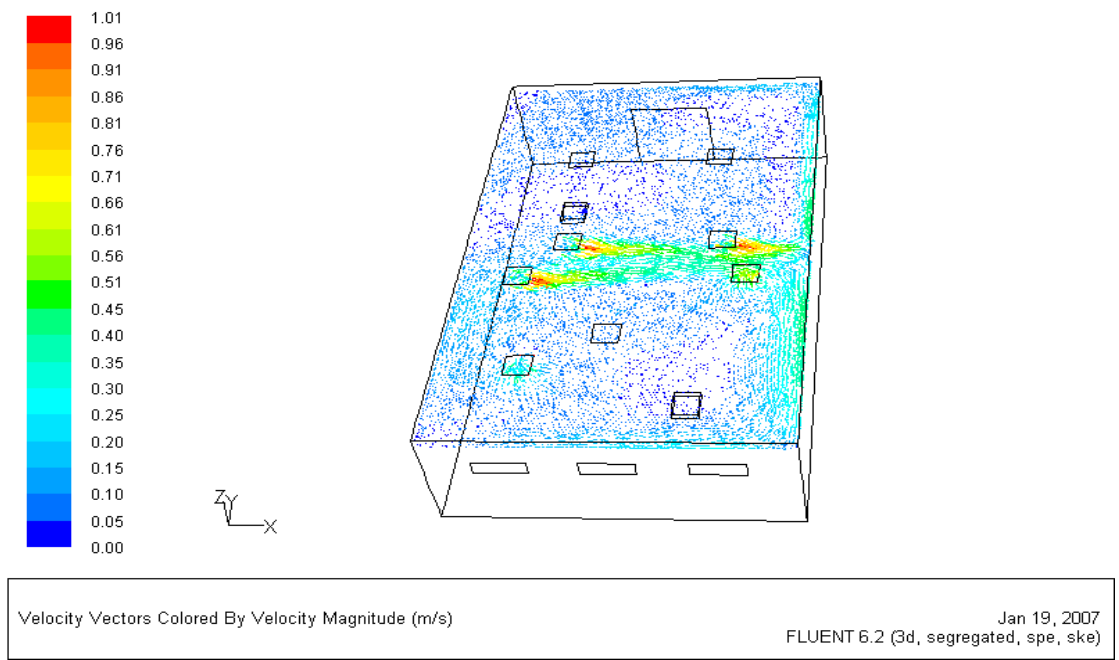
Fig.5. Horizontal velocity vector, Cut plan Z=2.8 m.

Contours of Velocity Magnitude (m/s)

Jan 19, 2007
FLUENT 6.2 (3d, segregated, spe, ske)
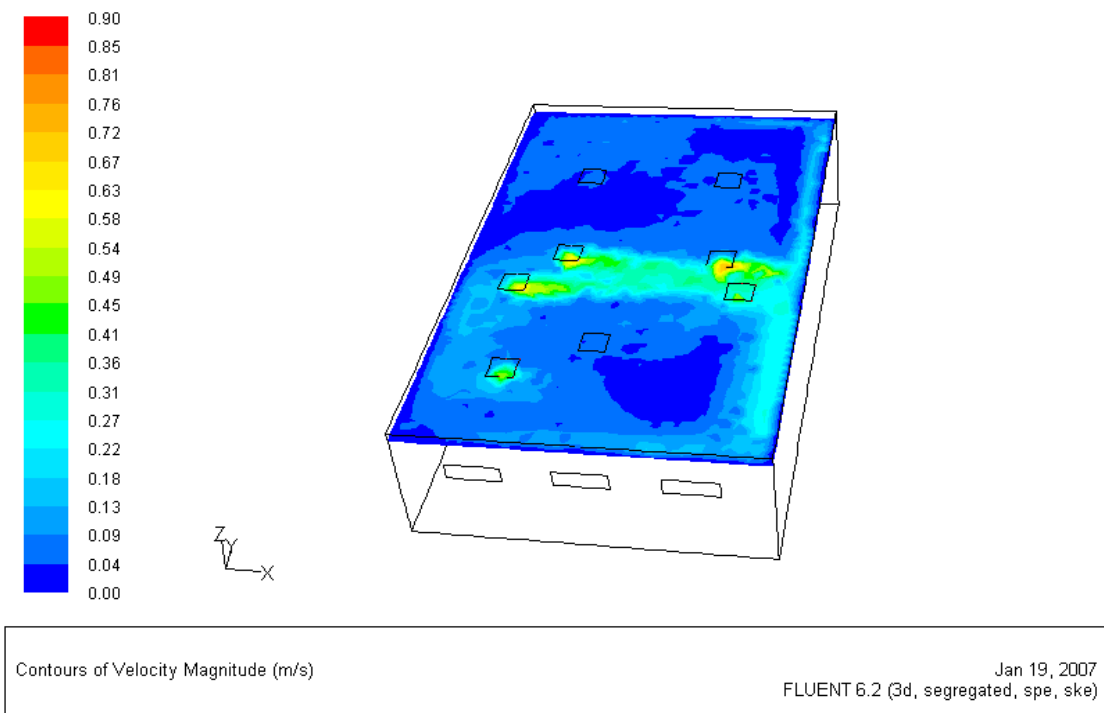
Fig.6. Velocity contour, Cut plan Z=2.8 m.

Contours of Static Temperature (k)   May 04, 2007
                                    FLUENT 6.2 (3d, segregated, spe, ske)
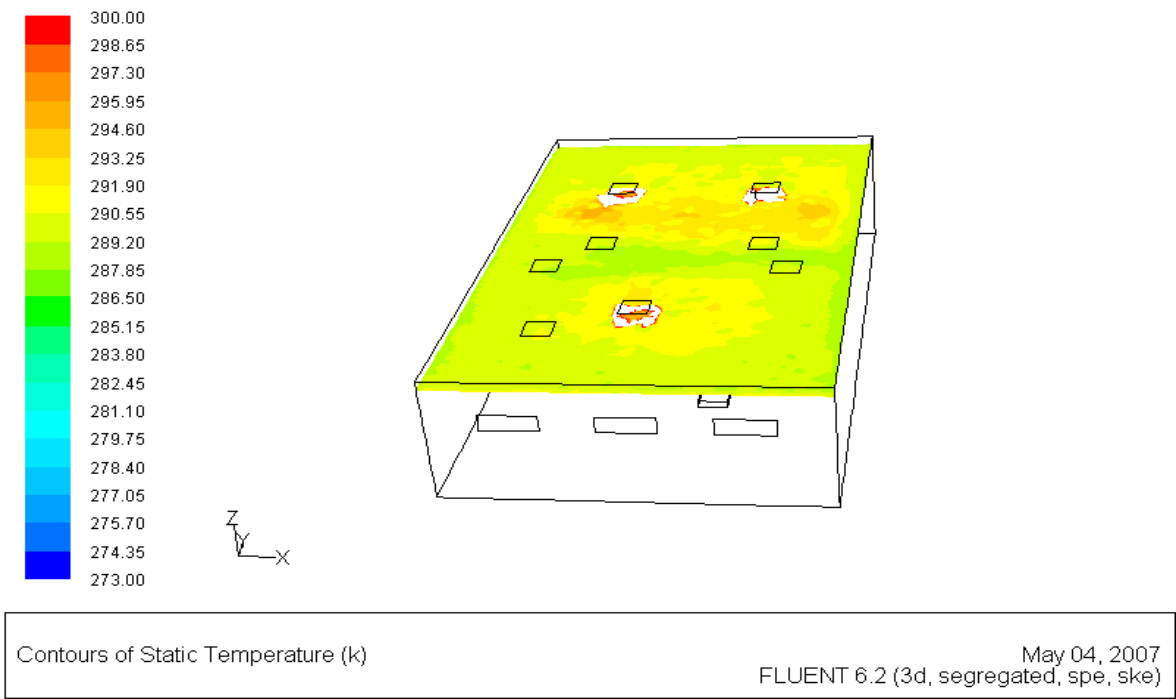
Fig.7. Isothermal contours, Cut plan Z=2.8 m.

Contours of Static Temperature (k)   May 04, 2007
                                    FLUENT 6.2 (3d, segregated, spe, ske)
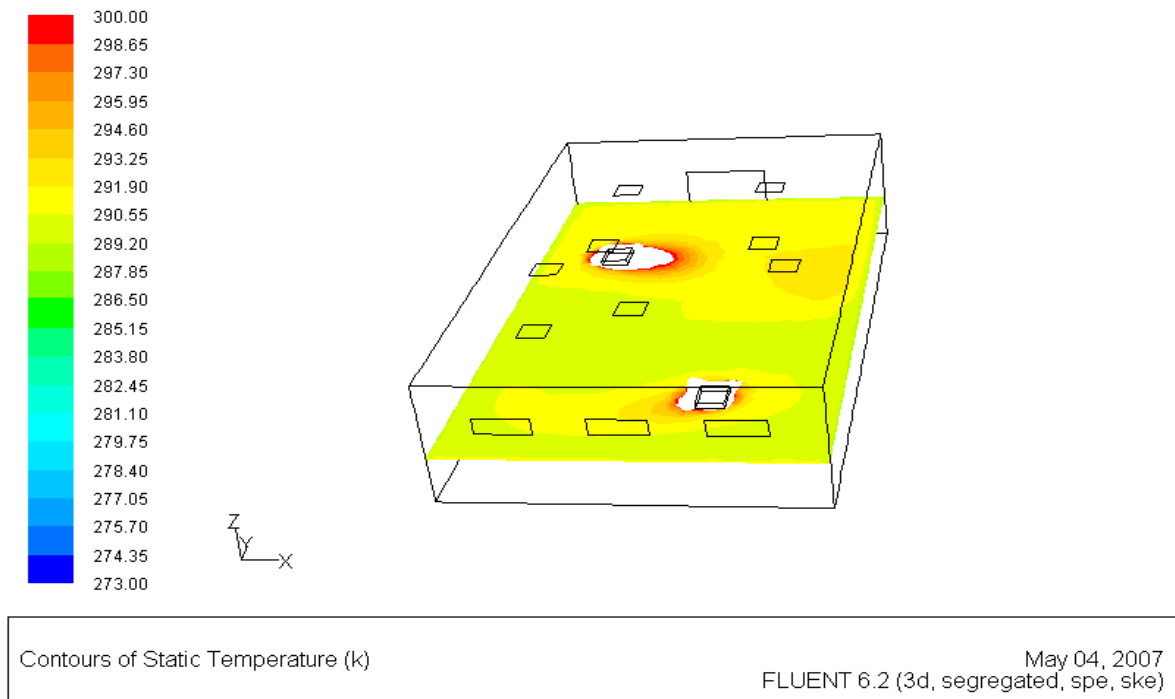
Fig.8. Isothermal contours, Cut plan Z=1.15 *m.*
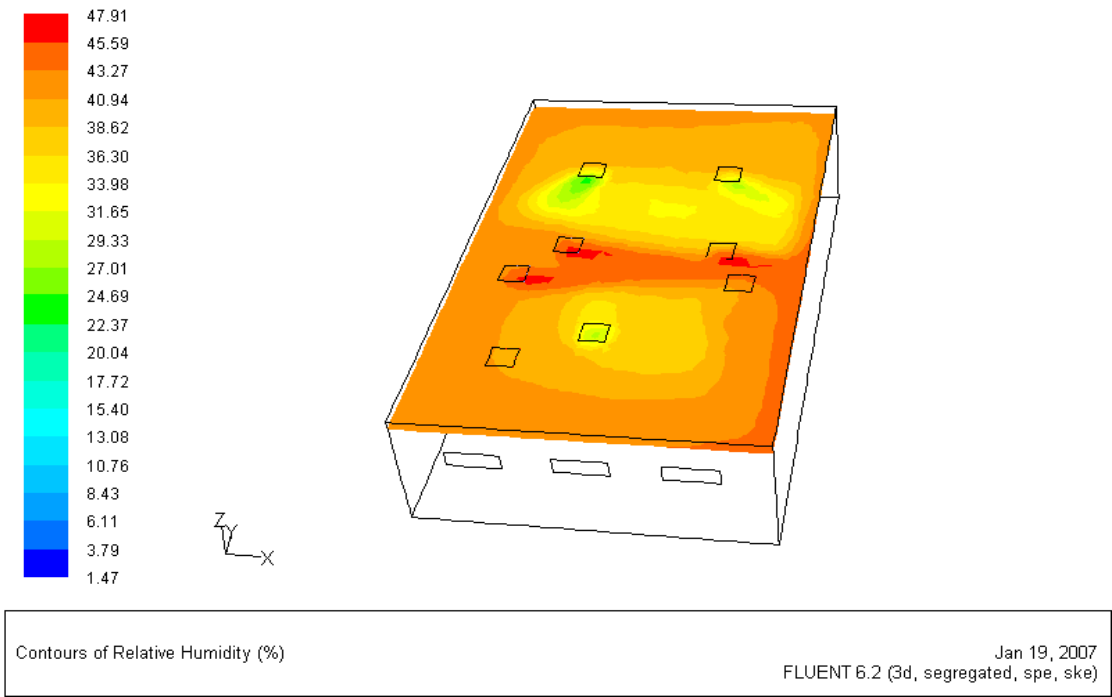
Fig.9. Relative humidity (R.H.%) contour, Cut plan Z=2.8 m.
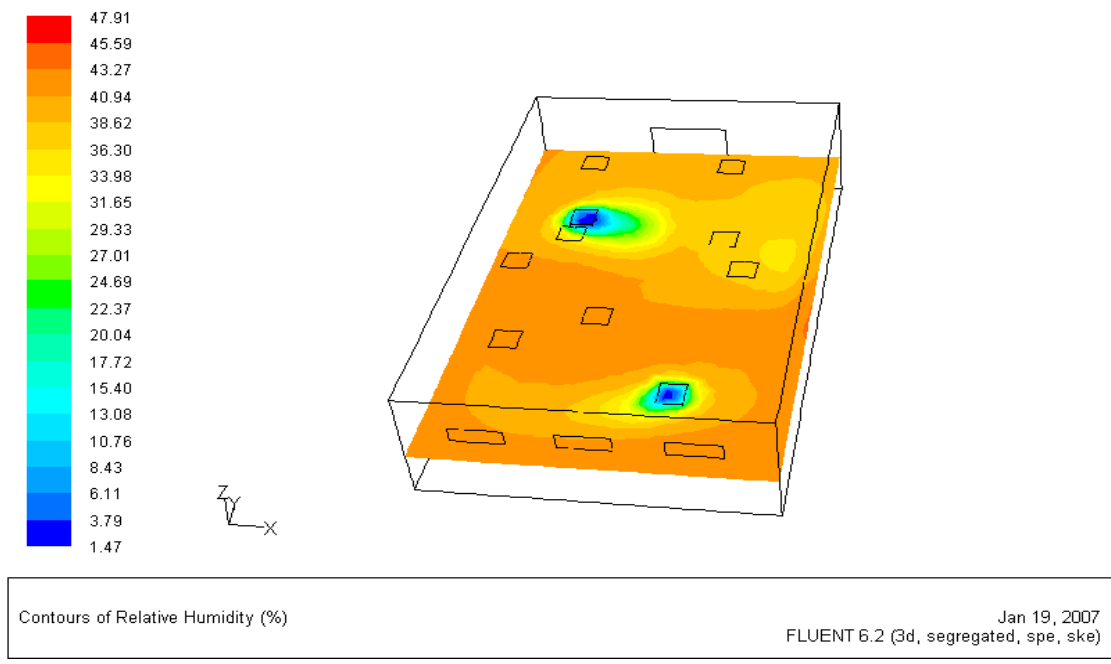
Fig.10. Relative humidity (R.H.%) contour, Cut plan Z=1.15 m.
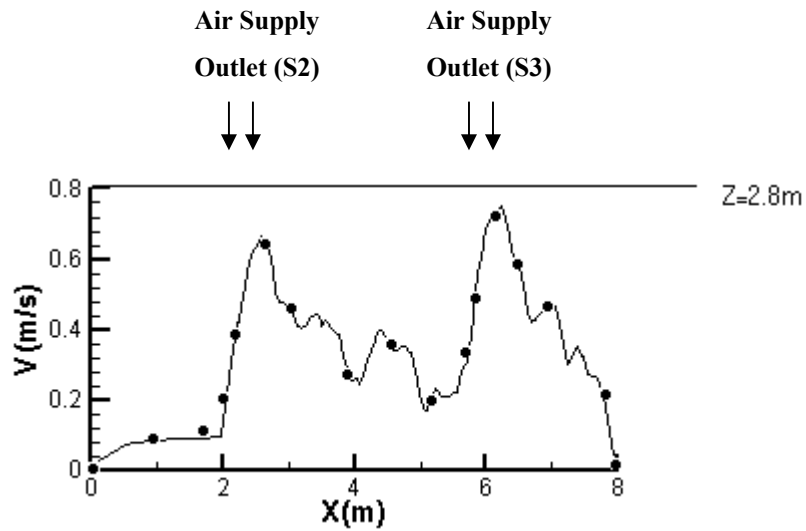
Air Supply
Outlet (S2)

Air Supply
Outlet (S3)

Fig.11. Comparison between Predicted and Measured Velocity profiles at various levels in the vicinity of supply diffusers, X-Z plan, Y=6.5m.

**Air Supply**
Outlet (S2)

Air Supply
Outlet (S3)

Fig.12. Comparison between Predicted and Measured Temperature profiles at various levels in the vicinity of supply diffusers, X-Z plan, Y=6.5m.

Air Supply
Outlet (S2)

Air Supply
Outlet (S3)
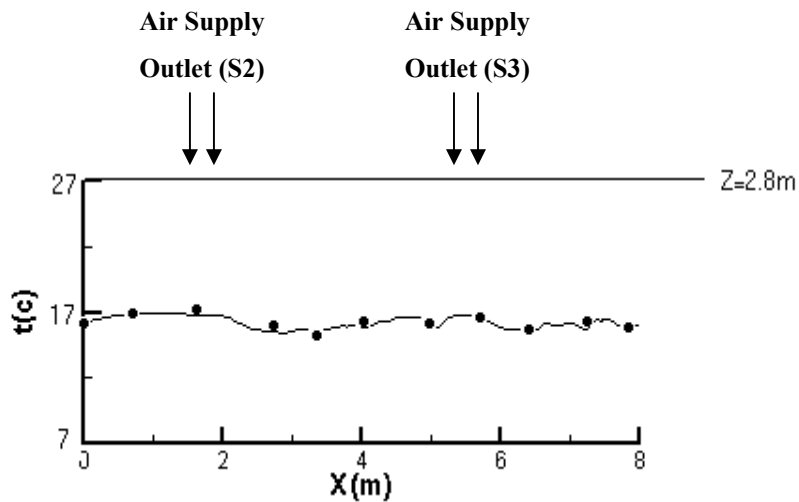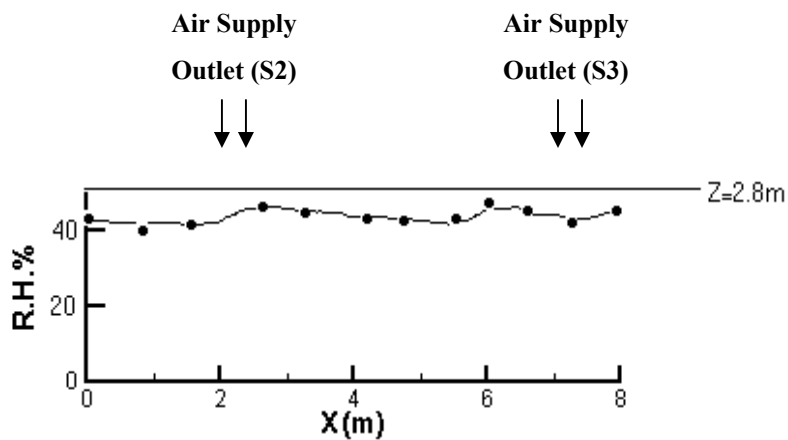
Fig.13. Comparison between Predicted and Measured Relative Humidity % profiles at various levels in the vicinity of supply diffusers, X-Z plan, Y=6.5m.
**Standard Device**
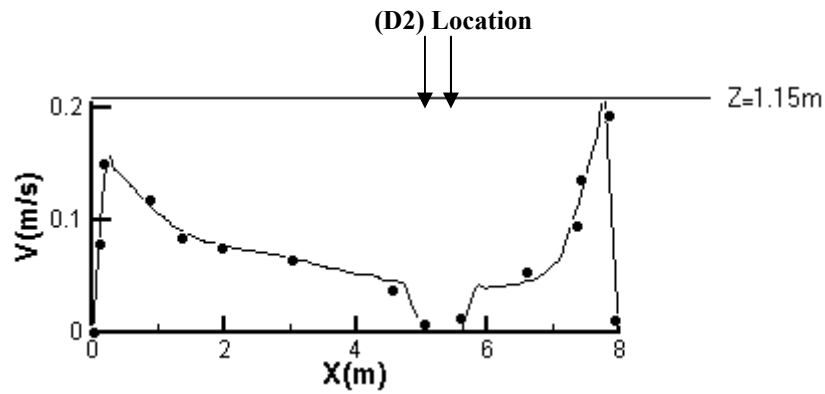
Fig.14. Comparison between Predicted and Measured Velocity profiles at various levels in the vicinity of the level of standard devices, X-Z plan, Y=10.5m.
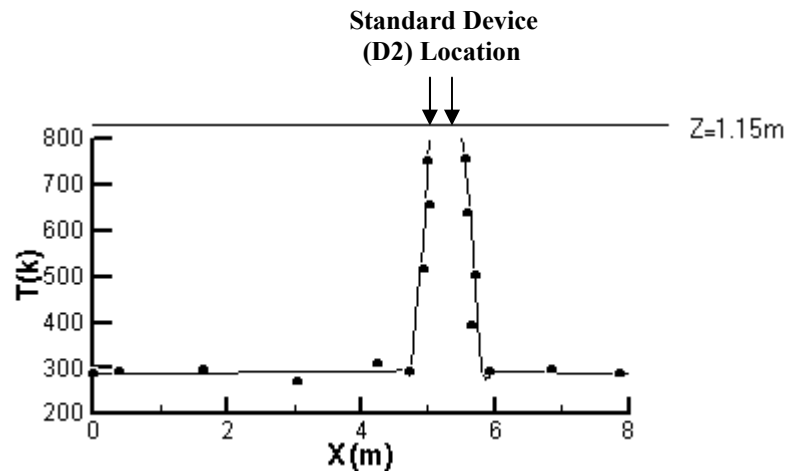

Fig.15. Comparison between Predicted and Measured Temperature profiles at various levels in the vicinity of the level of standard devices, X-Z plan, Y=10.5m.
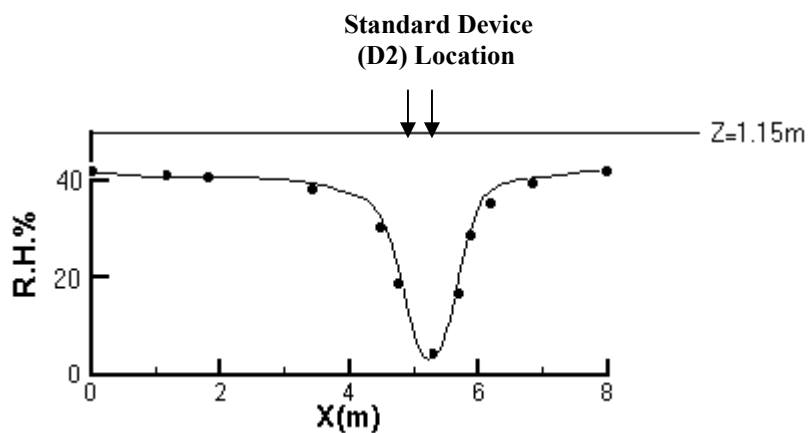

Fig.16. Comparison between Predicted and Measured Relative Humidity% profiles at various levels in the vicinity of the level of standard devices, X-Z plane=10.5m.